# COMPARISON OF NUMERICAL PHASE CHANGE MODELS IN TWO-PHASE HEAT TRANSFER PROBLEM

Jong Hyeon Son, Ho Lee, and Il Seouk Park*
*Author for correspondence
School of Mechanical Engineering,
Kyungpook National University,
Daegu, 41566,
Republic of Korea,
E-mail: einstein@knu.ac.kr

## ABSTRACT

This study focuses on a numerical simulation of phase change heat transfer between liquid and vapor. A numerical finite-volume approach was used to investigate the unsteady two-phase heat transfer problem. The initially saturated liquid or vapor is evaporated or condensed by the superheated or subcooled wall. The VOF (Volume Of Fluid) method is used to capture the interface of the saturated and unsaturated phases. The condensation and evaporation phenomenon at the liquid-vapor interface is numerically investigated by using the various interfacial mass and heat transfer models. Major differences in the phase change model are how to compute the heat transfer rate across the interface based on the temperature distributions near the interface during phase changing. In the present study, the existing phase change models are compared by solving the Stefan problem. The interfacial position, the temperature at a specific point and temperature profiles are illustrated over time and compared with analytic solutions.

## NOMENCLATURE

| | | |
|---|---|---|
| $c_p$ | [J/kgK] | Specific heat |
| $h_{lv}$ | [J/kg] | Latent heat |
| $k$ | [W/mK] | Thermal conductivity |
| $S_h$ | [W/m$^3$] | Heat source term |
| $t$ | [s] | Time |
| $T$ | [K] | Temperature |

Special characters

| | | |
|---|---|---|
| $\alpha$ | [-] | Volume fraction |
| $\delta$ | [m] | Film thickness |
| $\rho$ | [kg/m$^3$] | Density |

Subscripts

| | |
|---|---|
| $f$ | Cell face |
| $l$ | Liquid |
| $v$ | Vapor |
| $int$ | Interface cell |
| $uns$ | Unsaturated phase |
| $sat$ | Saturation |

## INTRODUCTION

During the phase change process of liquid and vapor phase, a large thermal energy can be transferred easily with large latent heat. In various industrial applications, the phase change phenomenon is widely applied for its high thermal performance. However theoretical and numerical analysis have been applied to a simple problem because the many complex physical phenomena are involved in the general problem [1-3].

To solve the phase change problem in many applications using the numerical methods, it is necessary to identify the characteristics of the numerical phase change model. Many phase change models have been suggested and modified. The existing phase change model is categorized into how to calculate the latent thermal energy by the phase change. There is the model using net heat flux around the interface cells proposed by Sato and Niceno [4] and Sun *et al.* [5]. And Lee [6] and Rattner and Garimella [7] suggested the phase change model calculating the latent thermal energy with the difference between the temperature of interface cell and saturation temperature of fluid. All phase change models estimate the mass and heat transfer rate from phase distributions and thermal information. But the process used to solve the temperature near the interfaces is different for each phase change model.

In this research, sharp interface model and Rattner and Garimella model are applied to one-dimensional Stefan problem. The phase change phenomenon including the mass and heat transfer through the interfaces is computed using the Volume Of Fluid method [8]. The time step and grid dependency of each model are handled. The position of the phase interface is compared to each phase change model.

## NUMERICAL METHOD

For the one-dimensional Stefan problem, the conservation equations of volume fraction and energy equation are used as a governing equation set,

$$\frac{\partial \alpha}{\partial t} = \frac{\dot{m}}{\rho} \tag{1}$$

$$\frac{\partial \left( \rho c_p T \right)}{\partial t} = \frac{\partial}{\partial x}\left( k \frac{\partial T}{\partial x} \right) + S_h \tag{2}$$

where, $\alpha$ is volume fraction, $t$ is time, $\dot{m}$ is mass transfer rate per unit volume, $\rho$ is density, $c_p$ is specific heat, $k$ is thermal conductivity, $T$ is temperature, $S_h$ is energy source per unit volume and subscripts $v$ and $l$ mean vapor and liquid respectively.

**Table 1** Iso-butane thermal properties

| Property | Liquid | Vapor |
|---|---|---|
| Density [kg/m$^3$] | 550.6 | 9.12 |
| Thermal conductivity [W/m·K] | 0.0892 | 0.0169 |
| Specific heat [J/kg·K] | 2446 | 1816 |
| Latent heat [J/kg] | 329400 | |

The sum of volume fractions for each phase is unity. The density and thermal conductivity used in the energy conservation equation (2) are the weight averages using the volume fraction of each phase.

$$\rho = \alpha_v \rho_v + \alpha_l \rho_l \tag{3}$$

$$k = \alpha_v k_v + \alpha_l k_l \tag{4}$$

The mass transfer rate per unit volume and energy source per unit volume is differently obtained for each phase change model. For the condensation problem, the equation for the liquid volume fraction is solved and the liquid density is used for the right-hand side of equation (2). In contrast, the vapor density is used for the evaporation problem

The volume fraction and energy equation is solved implicitly. The diffusion term in energy equation is discretized by the central differencing scheme. The two equations are two-way coupled.

The whole computational domain is 1 mm and initially filled with the saturated phase. The temperature at one end point is constant at subcooled temperature 5 K for the condensation. For the evaporation problem, the end point was kept at the superheated temperature 5 K. Other end point is maintained at the saturated temperature for both condensation and evaporation problems. In this study, the iso-butane is used for a working fluid. Thermal properties of iso-butane are listed in Table 1 and are constant.

In the present study, two different phase change model is used. One is the model based on the temperature difference between the local cell temperature and the saturated temperature. Rattner and Garimella [7] presented the following interfacial mass and heat transfer model:

$$S_h = \begin{cases} \min\{S_1, S_2, S_3\} & \text{for condensation} \\ \max\{-S_1, -S_2, -S_3\} & \text{for evaporation} \end{cases} \tag{5}$$

where $S_1$, $S_2$ and $S_3$ are defined as follows.

$$S_1 = \frac{\left(\rho C_p\right)_{eff}\left(T - T_{sat}\right)}{\Delta t} \tag{6}$$

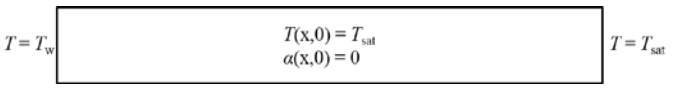


**Figure 1** Schematics of Stefan problem

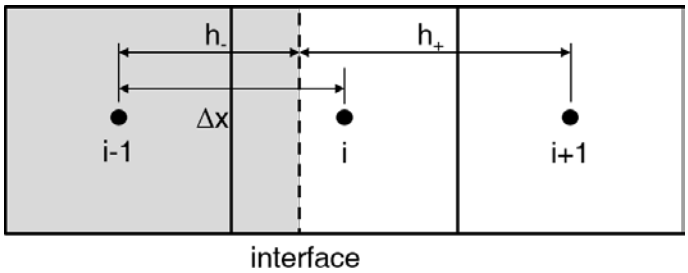


**Figure 2** Interface distance for the sharp interface model

$$S_2 = \begin{cases} \dfrac{\left(1-\alpha_l\right)\rho_v h_{lv}}{\Delta t} & \text{for condensation} \\ \dfrac{\alpha_l \rho_l h_{lv}}{\Delta t} & \text{for vaporization} \end{cases} \tag{7}$$

$$S_3 = \frac{h_{lv}}{\Delta t}\left(\frac{1}{\rho_v} - \frac{1}{\rho_l}\right)^{-1} \tag{8}$$

The $S_1$ is the heat source of calculating from the phase change amount for a single computing time interval ($\Delta$t); the phase change amount is obtained by the deviation from the saturation temperature. The $S_2$ represents the limit of the energy source since the phase change amount cannot exceed the amount of the saturated phase remaining in the cell. The $S_3$ is a device for numerical stability with limiting the growth rate of the interface.

The mass transfer rate per unit volume applied to the volume fraction equation (1) is calculated by the following equation:

$$\dot{m} = -\frac{S_h}{h_{lv}} \tag{9}$$

where $h_{lv}$ is the latent heat.

Second phase change model is based on the heat flux at the interfacial area. Sharp interface model [4] uses the total heat transfer amount in the interface cell instead of the temperature difference. In this model, the mass changing rate per unit volume is obtained from the heat transfer amount through the cell faces as following

$$\dot{m} = \frac{\sum_{faces} k_f \nabla T \cdot A_f}{h_{lv} \Delta V} \tag{10}$$

where, the $\Delta V$ is the cell volume. For one-dimensional Stefan problem, the interface area is equal to unity.

In sharp interface model, the source term in equation (2) is not included. The alternative method is used to fix the interface

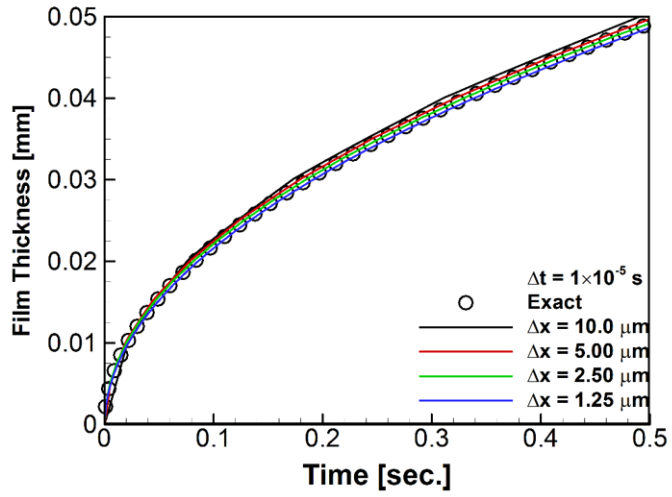


(a) Rattner and Garimella model

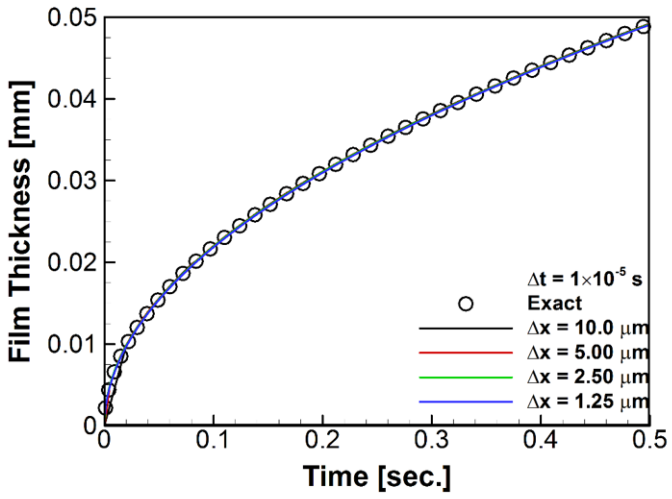


(b) Sharp interface

**Figure 3** The condensation film thickness for the different grid and the phase change model

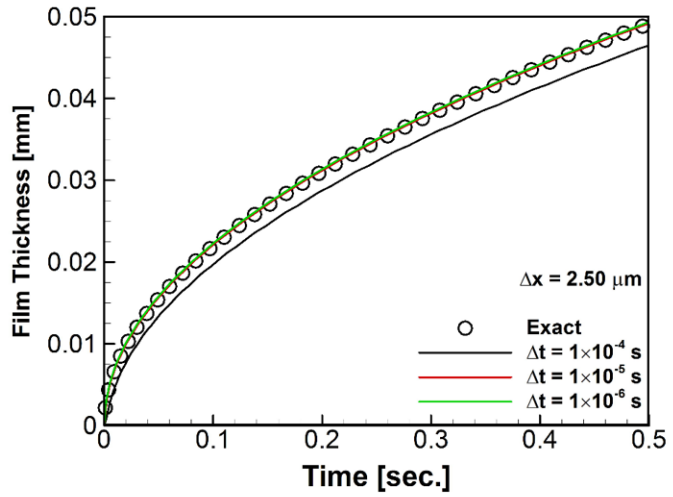


(a) Rattner and Garimella model

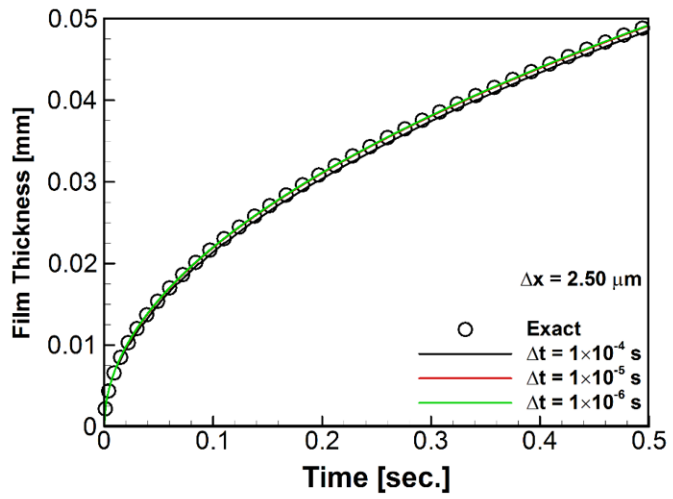


(b) Sharp interface

**Figure 4** The condensation film thickness for different time step size

cell temperature to saturated temperature. The temperature of the cell containing the interface is assumed to be the saturated temperature. Then, the interface distance between the interface and neighboring cell center is used for computing the gradient of temperature as shown in Fig. 2. As a result, the interface cell is numerically computed as a Dirichlet boundary condition maintained at the saturated temperature.

The exact solution [9] of film thickness for unsaturated phase and temperature distribution could be obtained by the following equation,

$$\chi \exp\left(\chi^2\right)\mathrm{erf}\left(\chi\right)=\frac{c_p\left(T_{wall}-T_{sat}\right)}{h_{lv}\sqrt{\pi}} \tag{11}$$

$$\delta\left(t\right)=2\chi\sqrt{\frac{k}{\rho c_p}t} \tag{12}$$

$$T\left(x,t\right)=T_{wall}+\left(\frac{T_{sat}-T_{wall}}{\mathrm{erf}\left(\chi\right)}\right)\mathrm{erf}\left(\frac{x}{2\sqrt{\Gamma_G t}}\right) \tag{13}$$

for $0\le x\le\delta\left(t\right)$

where $\chi$ is a solution of the transcendental equation, and erf is an error function.

## RESULTS

Fig. 3 shows the grid dependency for the phase change model. The results of condensation film thickness for time change are compared with the exact solution when the time step size is $10^{-5}$ sec. For the Rattner and Garimella model, the amount of liquid condensed is reduced with increasing the grid number. For the case of sharp interface model, the film thickness for the grid number show the same results. And there is very little difference between the exact solutions.

The time step size test for the phase change model is conducted. As shown in Fig. 4, the Rattner and Garimella

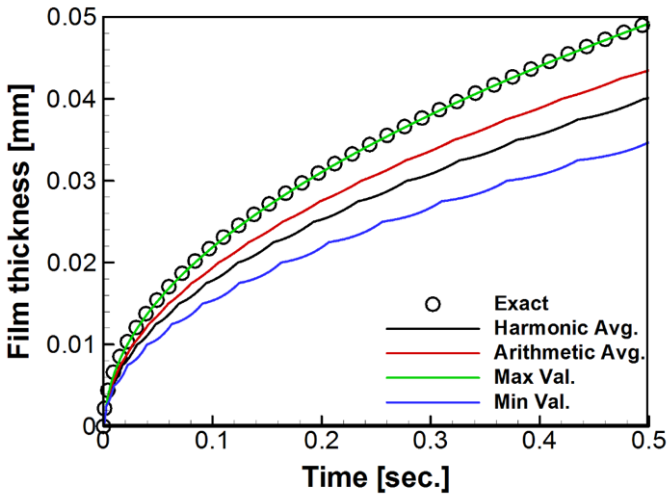


(a) Film thickness

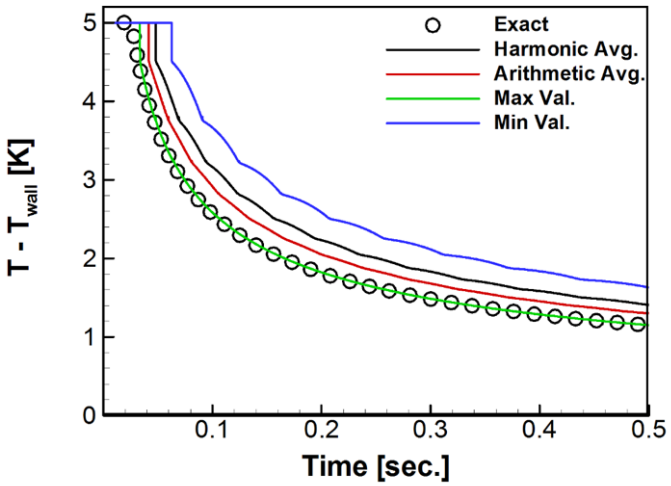


(b) Temperature

**Figure 5** The condensed film thickness and temperature histories for the cell face thermal conductivity

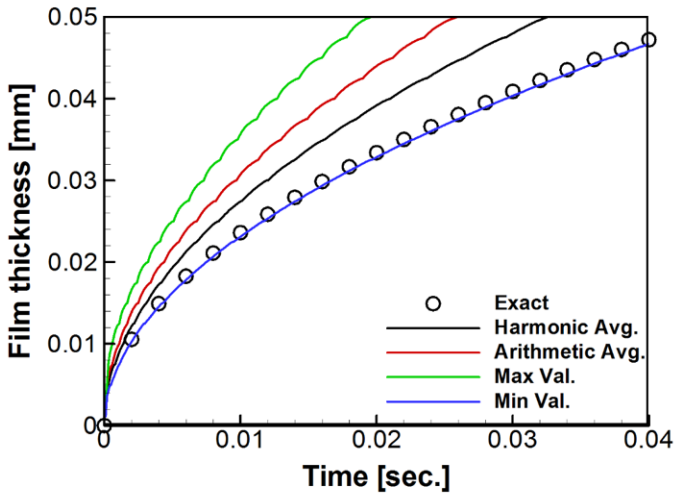


(a) Film thickness

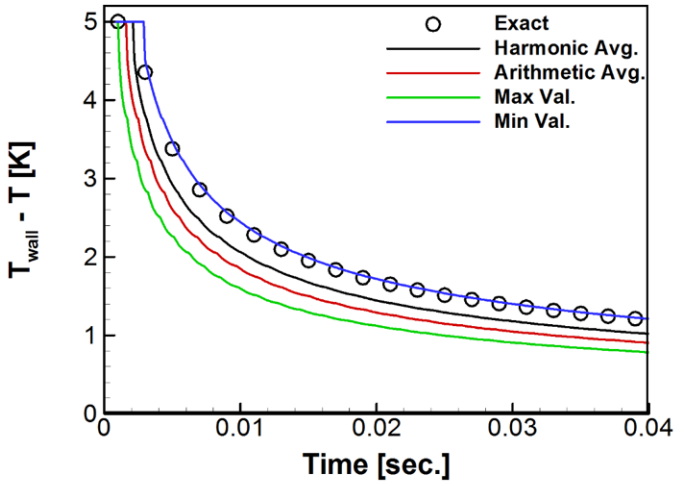


(b) Temperature

**Figure 6** The evaporated film thickness and temperature histories for the cell face thermal conductivity

model computed the amount of condensation less than the amount of the sharp interface model when the time step size is $10^{-4}$ sec. For the sharp interface model, there is less difference in the film thickness with decreasing the time step size. As time step size is reduced, the condensation film thickness for both model is almost same with the exact solution.

Fig. 5 shows the film thickness and temperature histories at the fixed point near the wall according to the calculation method of thermal conductivity at the cell face of interface cell. Because the properties of cells are very different through the cell face, it is important to set the cell face properties appropriately for numerical stability. Four methods to set the face value of thermal conductivity are tested along with the sharp interface model.

Harmonic average:

$$k_f^{-1} = k_{\text{uns}}^{-1} + k_{\text{int}}^{-1} \tag{14}$$

Arithmetic average:

$$k_f = \left(k_{\text{uns}} + k_{\text{int}}\right)/2 \tag{15}$$

Maximum value:

$$k_f = \max\left\{k_{\text{uns}}, k_{\text{int}}\right\} \tag{16}$$

Minimum value:

$$k_f = \min\left\{k_{\text{uns}}, k_{\text{int}}\right\} \tag{17}$$

Except for the case of the maximum value, the amount of phase changing is less than the exact solution. The cell-face value changes every time step because of the volume fraction of interface cell change by the source term. According to these change, the mass transfer rate gradually increases when the volume fraction is close to unity. The temperature change over

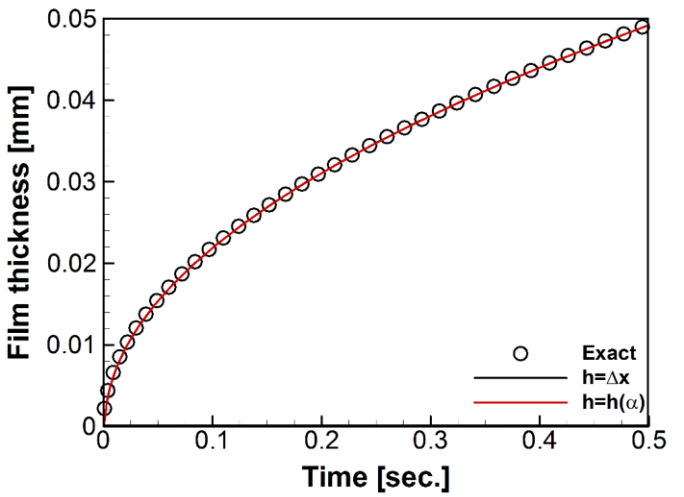


(a) Film thickness

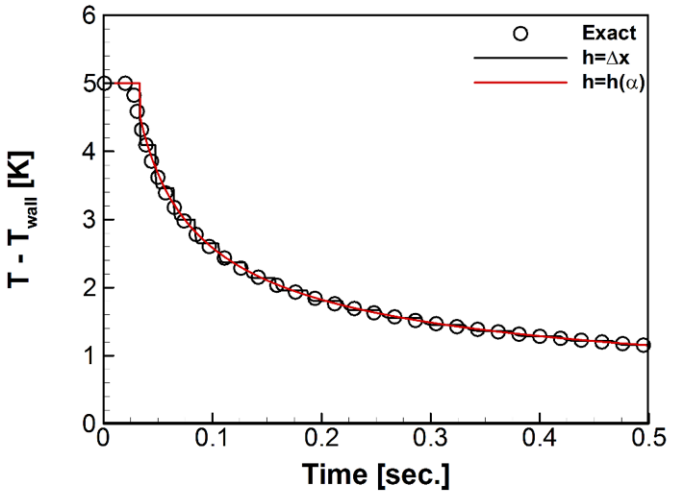


(b) Temperature

**Figure 7** Film thickness and temperature change over time according to the interface distance

time is not smooth because of the time-dependent thermal conductivity. The method to choice the minimum value of liquid phase and interface cell value is also not suitable for condensation Stefan problem. For condensation problem, the thermal conductivity of cell face has to set to the value of liquid phase.

To solve the evaporation Stefan problem, the thermal conductivity of vapor phase should be used for the value at the cell face as shown in Fig. 6. The results of film thickness for other setting method show that the amount of phase change is calculated excessive. Unlike the condensation problem, when the maximum value is selected, the selected value gradually increase at each time step because the thermal conductivity of the interface cell is larger than that of the vapor phase. Also except the case of selecting the minimum value, the thermal conductivity of the cell face abruptly changes when the position of the interface cell moves to the next cell. As a result, as shown in Fig. 6 the film thickness and the temperature change unevenly.

Fig. 7 show the effect of interface distance for sharp interface model on the phase change. The results show that the film thickness is not affected by the interface distance because the movement of the interface in the cell is negligible as the grid spacing decreases. But the temperature change for time progression at a certain point is affected by interface distance. The results show step-wise change unlike changes in the film thickness. As the interface position pass the cell face, the temperature steeply changes. And the temperature not changes during a certain period of time.

## CONCLUSIONS

Using the one-dimensional Stefan problem, the characteristics of the numerical model of phase change has been investigated. The model using the heat fluxes through cell faces to calculate the amount of phase change, showed better agreement with exact solutions in terms of the interfacial position and temperature histories. It was found that the selecting the diffusion coefficient on cell faces properly was essential; the using the diffusion coefficient for unsaturated phase gives more accurate results regardless the evaporation and condensation.

## REFERENCES

[1] Da Riva E., and Del Col DNumerical simulation of laminar liquid film condensation in a horizontal circular minichannel, *Journal of Heat Transfer*, Vol. 134, 2012, 051019.

[2] Chen S., Zhen Y., Duan Y, and Wu D., Simulation of condensation flow in a rectangular microchannel, *Chemical Engineering and Processing*, Vol. 76, 2014, pp. 60-69.

[3] Bahreini M., Ramiar A., and Ranjbar A. A., Numerical simulation of bubble behaviour in subcooled flow boiling under velocity and temperature gradient, *Nuclear Engineering and Design*, Vol. 293, 2015, pp. 238-248.

[4] Sato Y., and Niceno B., A sharp-interface phase change model for a mass-conservative interface tracking method, *Journal of Computational Physics*, Vol. 249, 2013, pp. 127-161

[5] Sun D., Xu J., and Chen Q., Modeling of the evaporation and condensation phase-change problems with FLUUENT, *Numerical Heat Transfer, Part B*, Vol. 66, 2014, pp. 326-342

[6] Lee W. H., Pressure iteration scheme for two-phase flow modeling, *Multiphase transport: Fundamentals, Reactor safety, Applications*, Hemisphere Publishing, Washington DC, 1980

[7] Rattner A. S., and Garimella S., Simple mechanistically consistent formulation for Volume-of-Fluid based computations of condensing flows, *Journal of Heat and Mass Transfer*, Vol. 136, 2014, 071501

[8] Hirt C. W., and Nichols B. D., Volume of fluid (VOF) method for the dynamics of free boundaries, *Journal of Computational Physics*, Vol. 39, 1981, pp. 201-225

[9] Alexiades V., and Solomon A. D., *Mathematical modeling of melting and freezing processes*, Hemisphere, Washington, DC, 1993.